Electronic Supplementary Material (ESI) for Medicinal Chemistry Communications

Supplementary Information

Flavans from *Desmos cochinchinensis* as potent aromatase inhibitors

Vilailak Prachyawarakorn, Suwannee Sangpetsiripan, Panida Surawatanawong, Chulabhorn Mahidol, Somsak Ruchirawat, and Prasat Kittakoop

Table S1. Cytotoxicity of compounds **1-8**.

Compound	Cytotoxic activity, IC_{50} (μM), mean±s.d. (n = 3)			
	MOLT-3	HepG-2	A549	HuCCA-1
1	24.33±4.57	Inactive	146.67±7.07	130.00±16.50
2	57.41±6.98	99.60±11.55	137.20±0.00	Inactive
3	63.50±10.73	135.35±11.27	Inactive	Inactive
4	41.27±7.23	Inactive	Inactive	140.13±6.75
5	29.81±2.90	143.31±15.92	Inactive	143.31±0.00
6	28.48±2.93	144.81±10.79	103.66±15.09	125.00±4.31
7	71.98±5.97	Inactive	Inactive	Inactive
8	ND	ND	ND	ND
Etoposide[a]	0.03±0.01	22.11±4.81	ND	ND
Doxorubicin[a]	ND	0.50±0.11	0.90±0.03	1.10±0.26

[a]Etoposide and doxorubicin are standard drugs.
ND = not determined

Table S2. The binding energies calculated by Autodock Vina.

Compound[a]	Rigid binding energy (kcal/mol)	Flexible binding energy (kcal/mole)
1	–8.1	–8.5
2	–6.3	–7.3
3	–6.3	–8.0
4	–7.5	–8.5
5	–7.8	–8.5
6	–7.4	–8.3
Formestane	–13.1	–13.4
Andromestenedione	–13.6	–13.7
Andromestenedione (X-ray)	–13.9	–14.1

[a] Geometry optimization by B3LYP/6-31G(d)

Binding of androstenedione and formestane

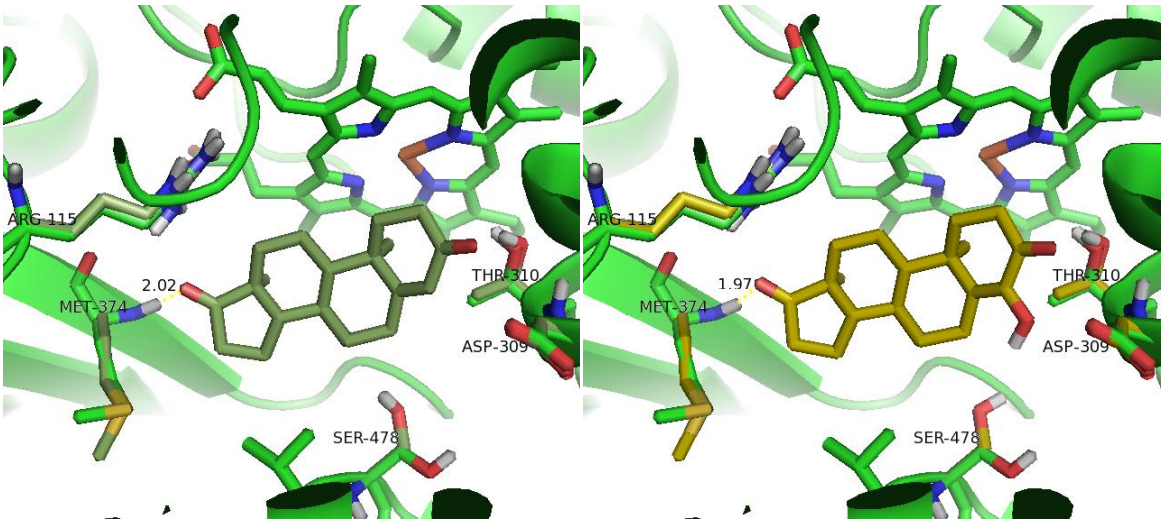

A **B**

Fig. S1. Lowest energy poses of andromestenedione (A) and formestane (B), within the aromatase binding site. The crystal structure is in bright green. The flexible residues are Met374, Arg115, Thr310, Ser478, and Asp309. Due to the flexible docking, some atoms change from their starting positions (shown in dark green and dark yellow). The ligand structures were optimized by B3LYP/6-31G(d).

Binding of inhibitors 2 and 3

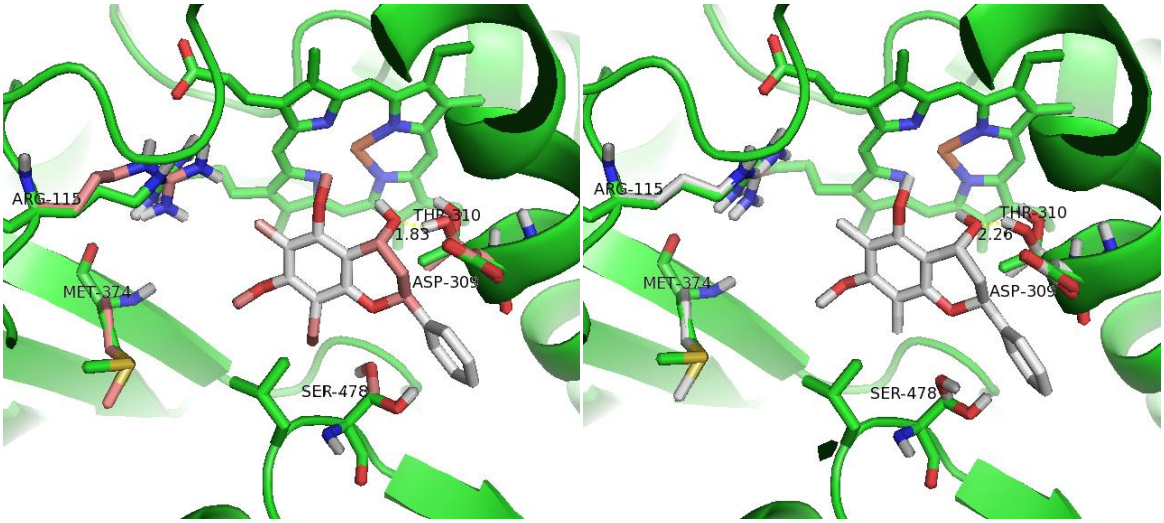

A **B**

Fig. S2. Lowest energy poses of aromatase inhibitors **2** (A) and **3** (B), within the aromatase binding site. The crystal structure is in bright green. The flexible residues are Met374, Arg115, Thr310, Ser478, and Asp309. Due to the flexible docking, some atoms change from their starting positions (shown in pale pink and in dark grey). The ligand structures were optimized by B3LYP/6-31G(d).

Fig. S3. ^{1}H NMR spectrum ($CDCl_3$) of compound **1**

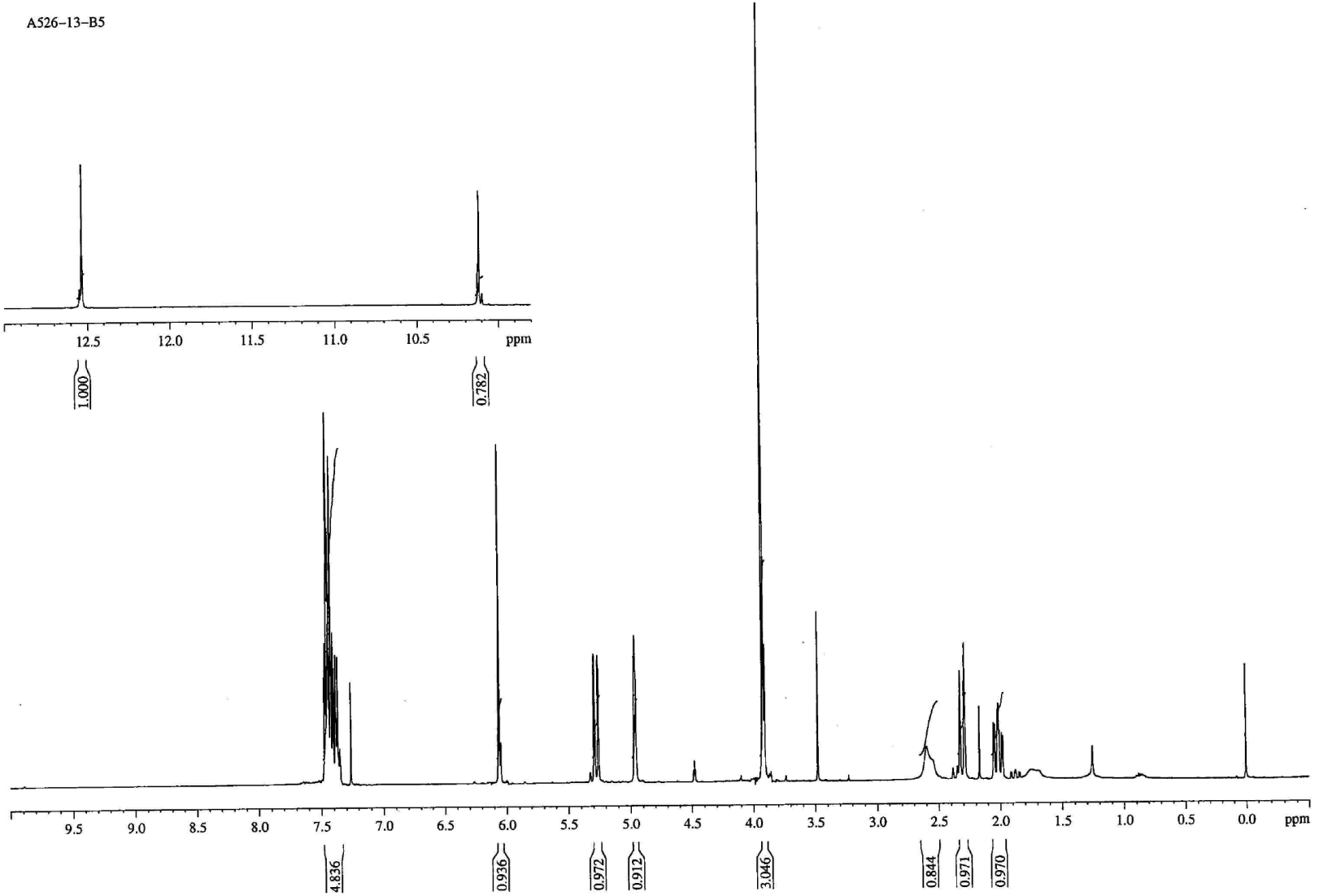

Fig. S4. ^{13}C NMR spectrum ($CDCl_3$) of compound **1**

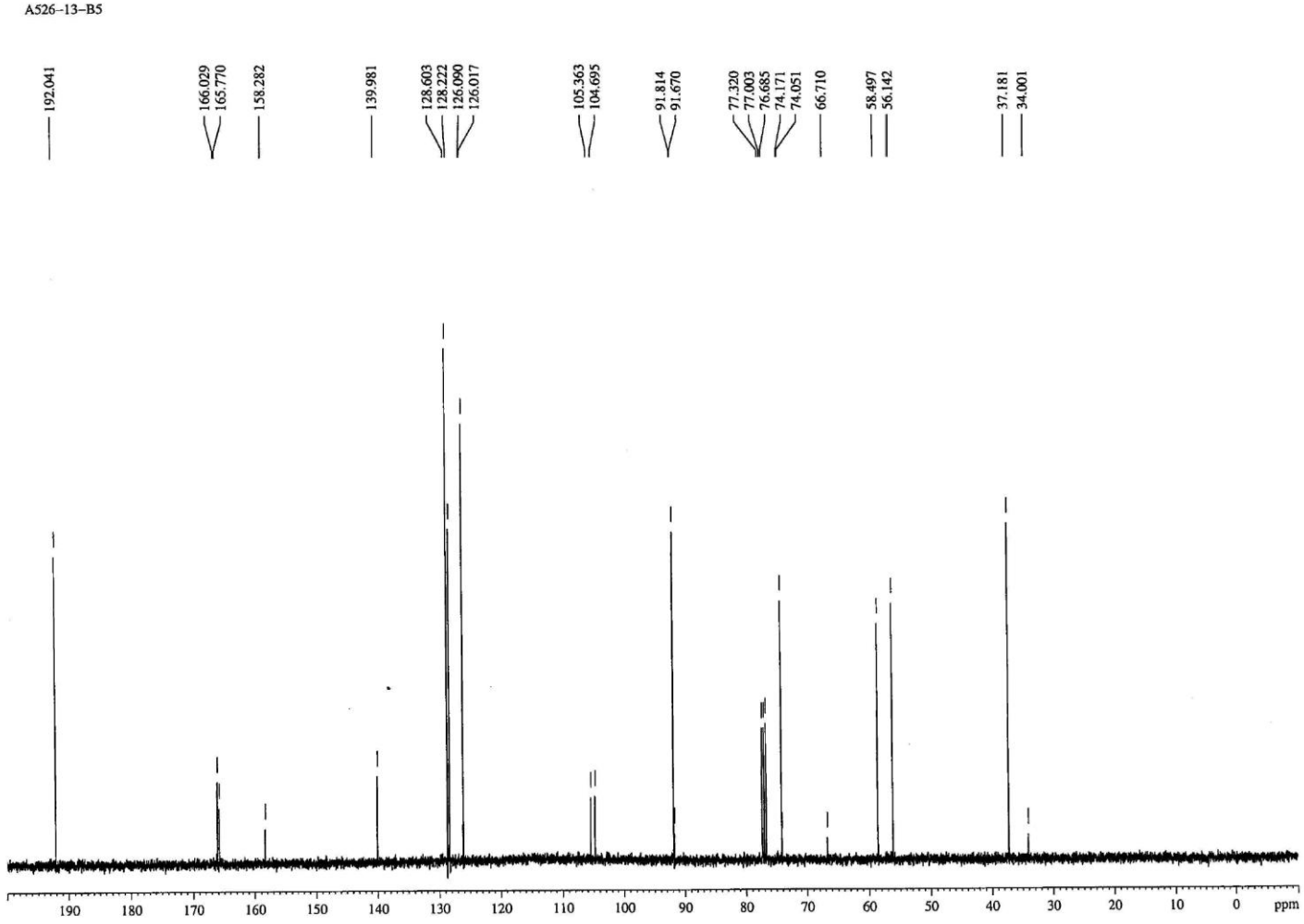

Fig. S5. HMQC spectrum of compound **1**

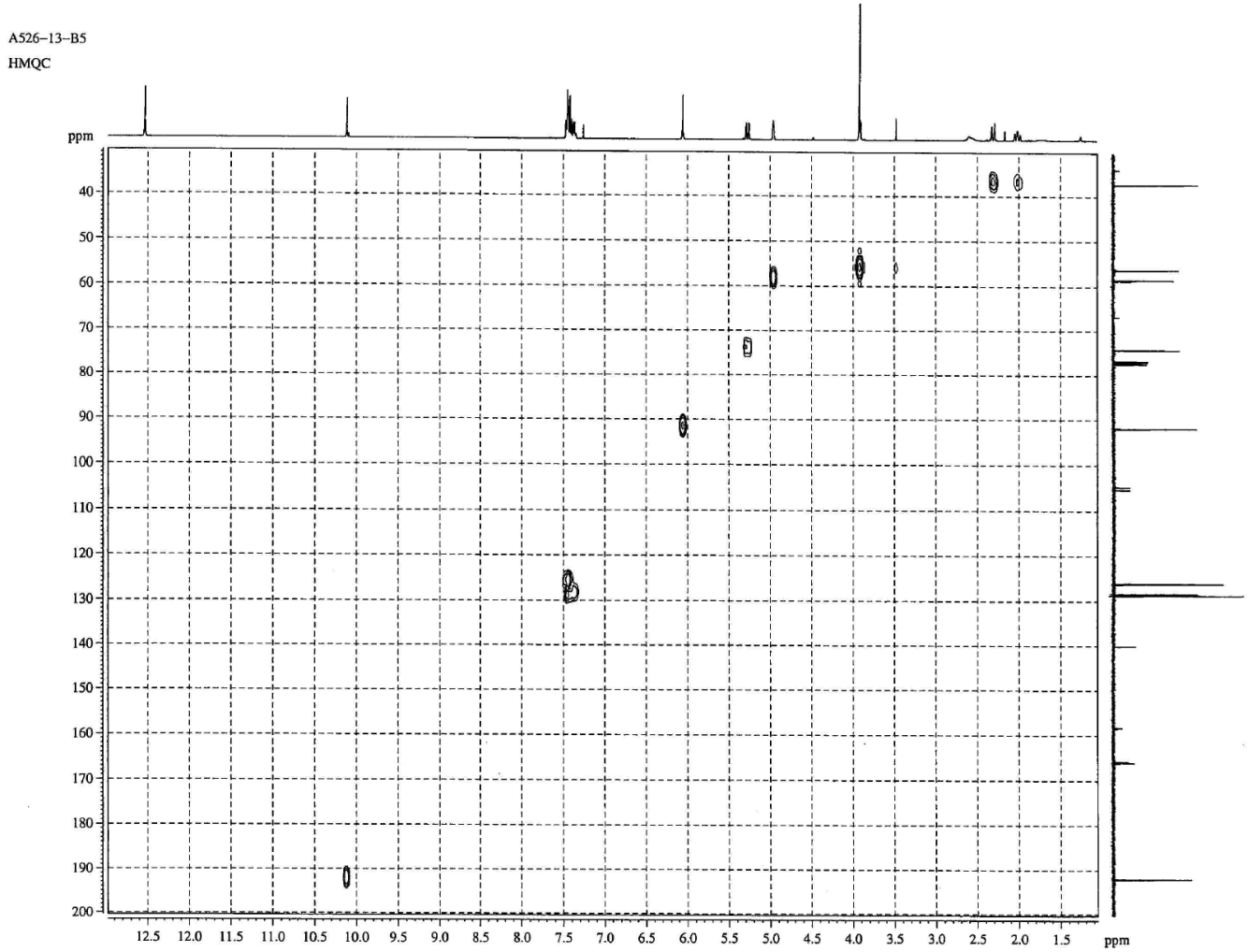

Fig. S6. HMBC spectrum of compound **1**

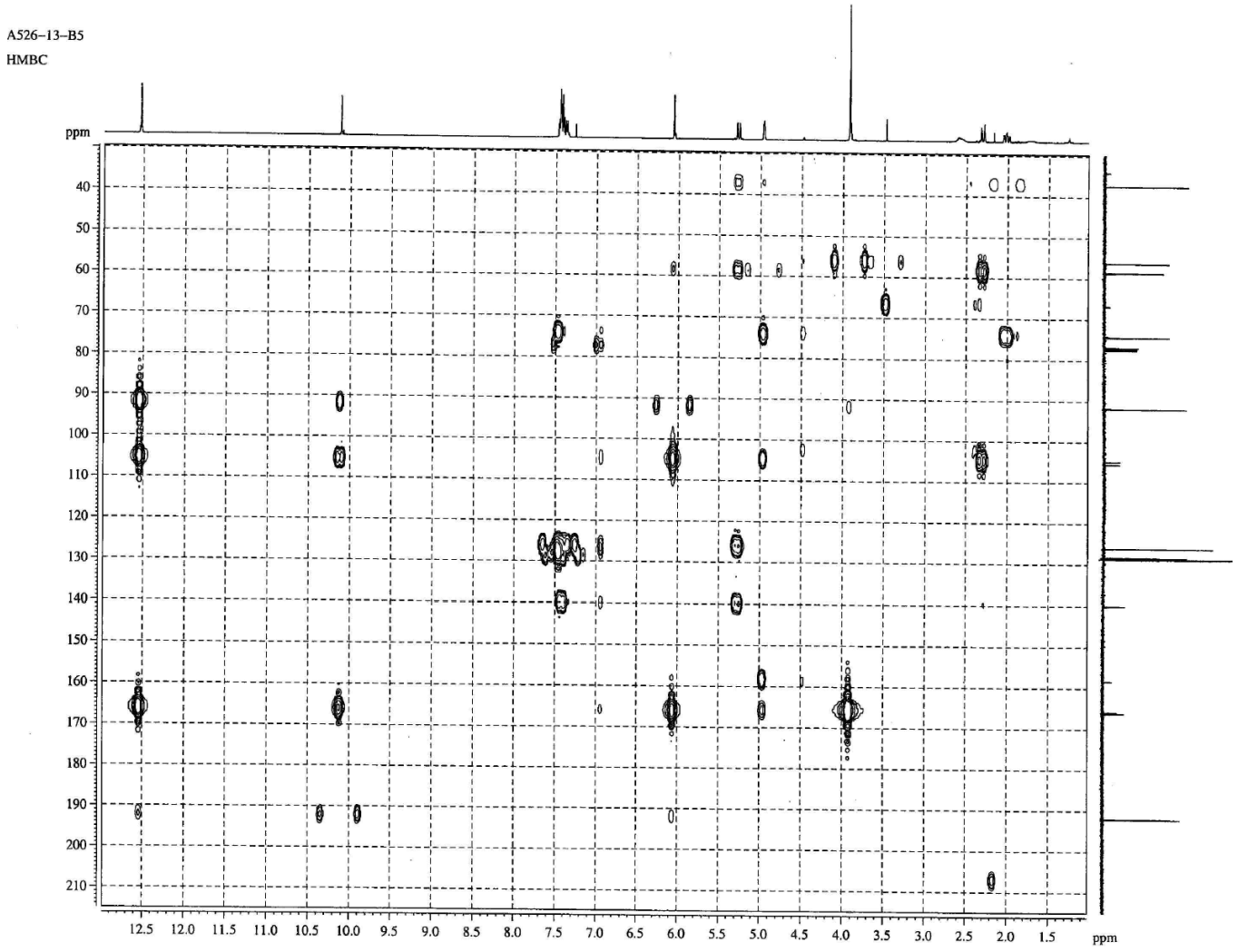

Fig. S7. ^{1}H NMR spectrum ($CDCl_3$) of compound **2**

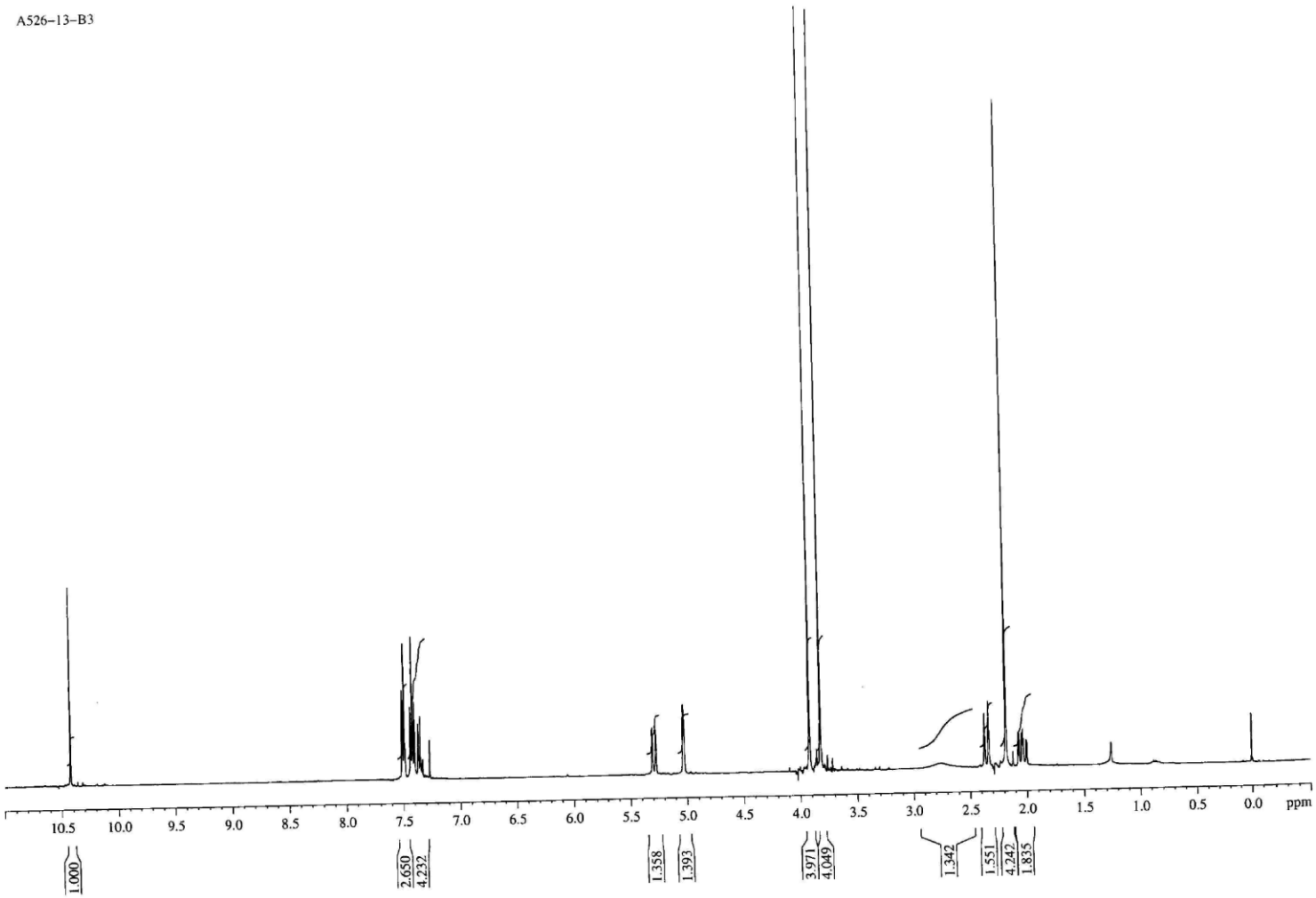

Fig. S8. ^{13}C NMR spectrum ($CDCl_3$) of compound **2**

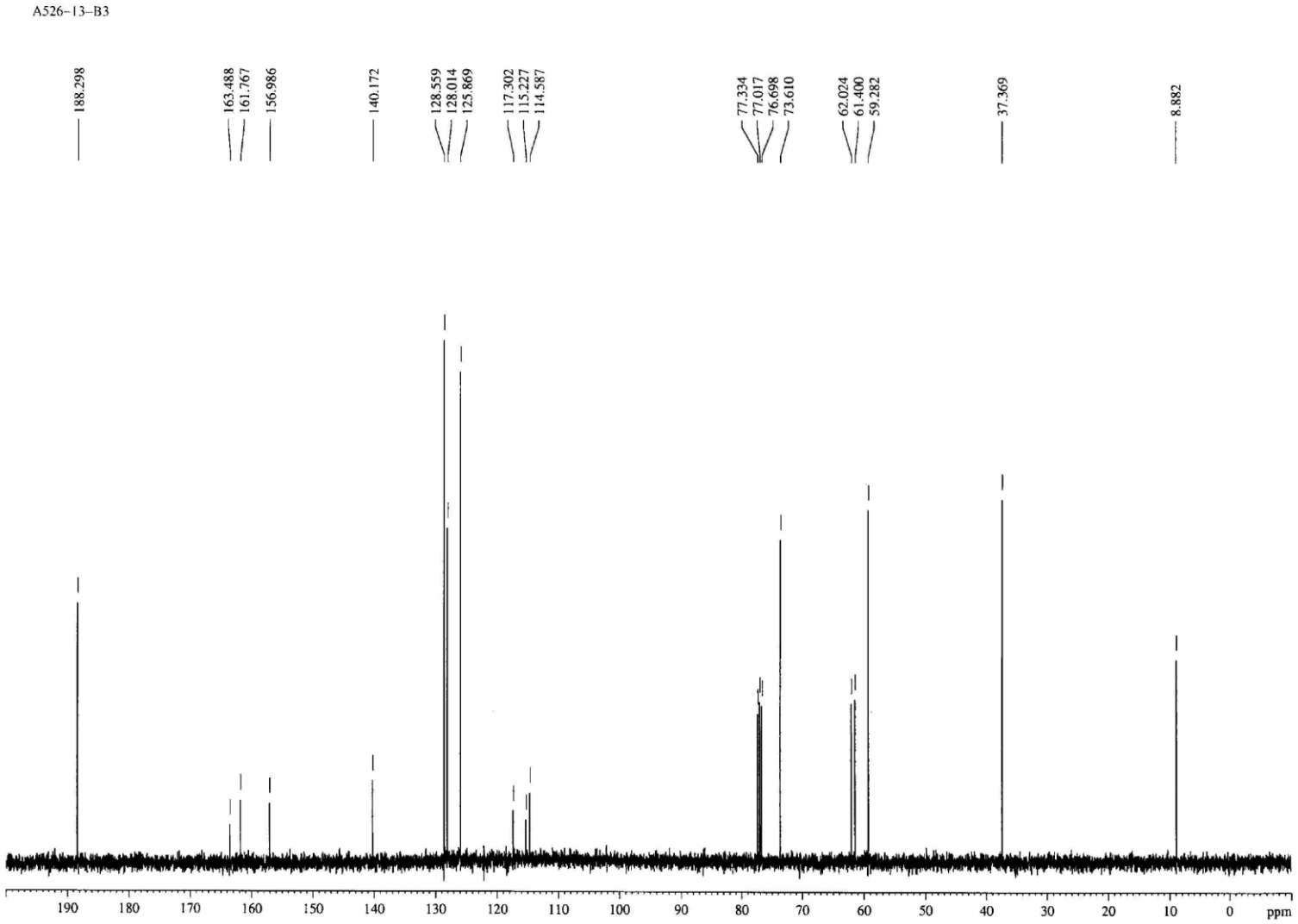

Fig. S9. HMQC spectrum of compound **2**

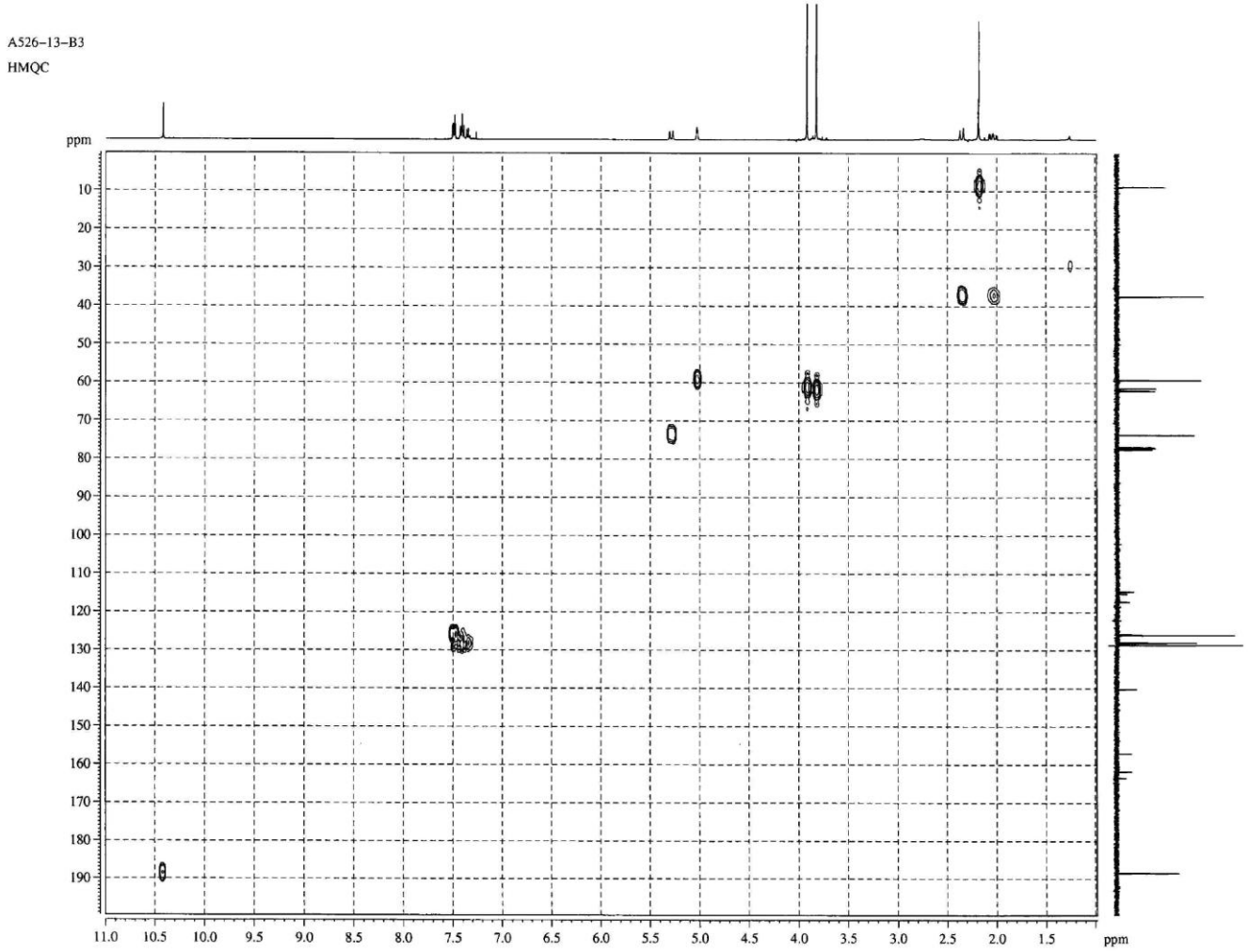

Fig. S10. HMBC spectrum of compound **2**

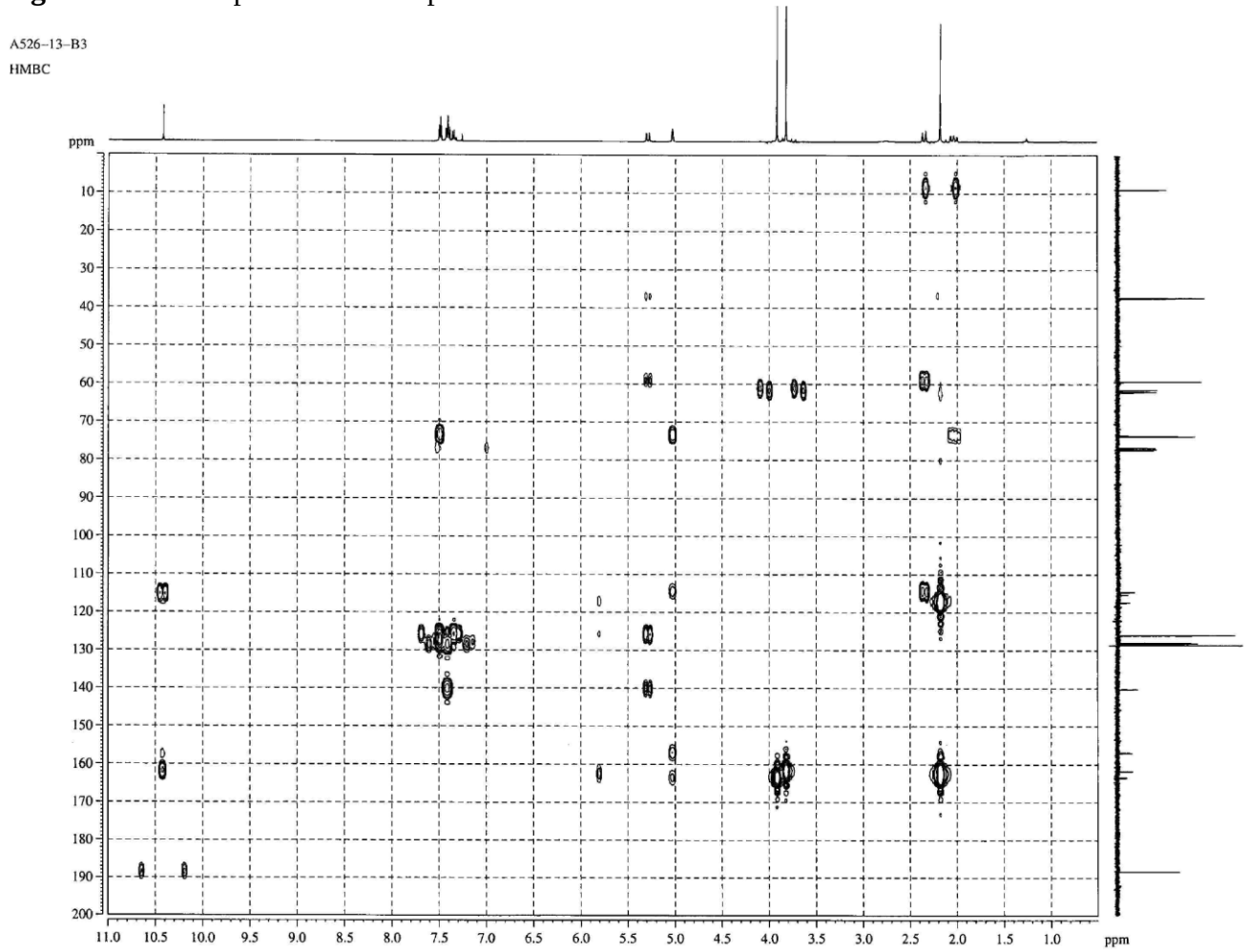

Fig. S11. ^{1}H NMR spectrum ($CDCl_3$) of compound **3**

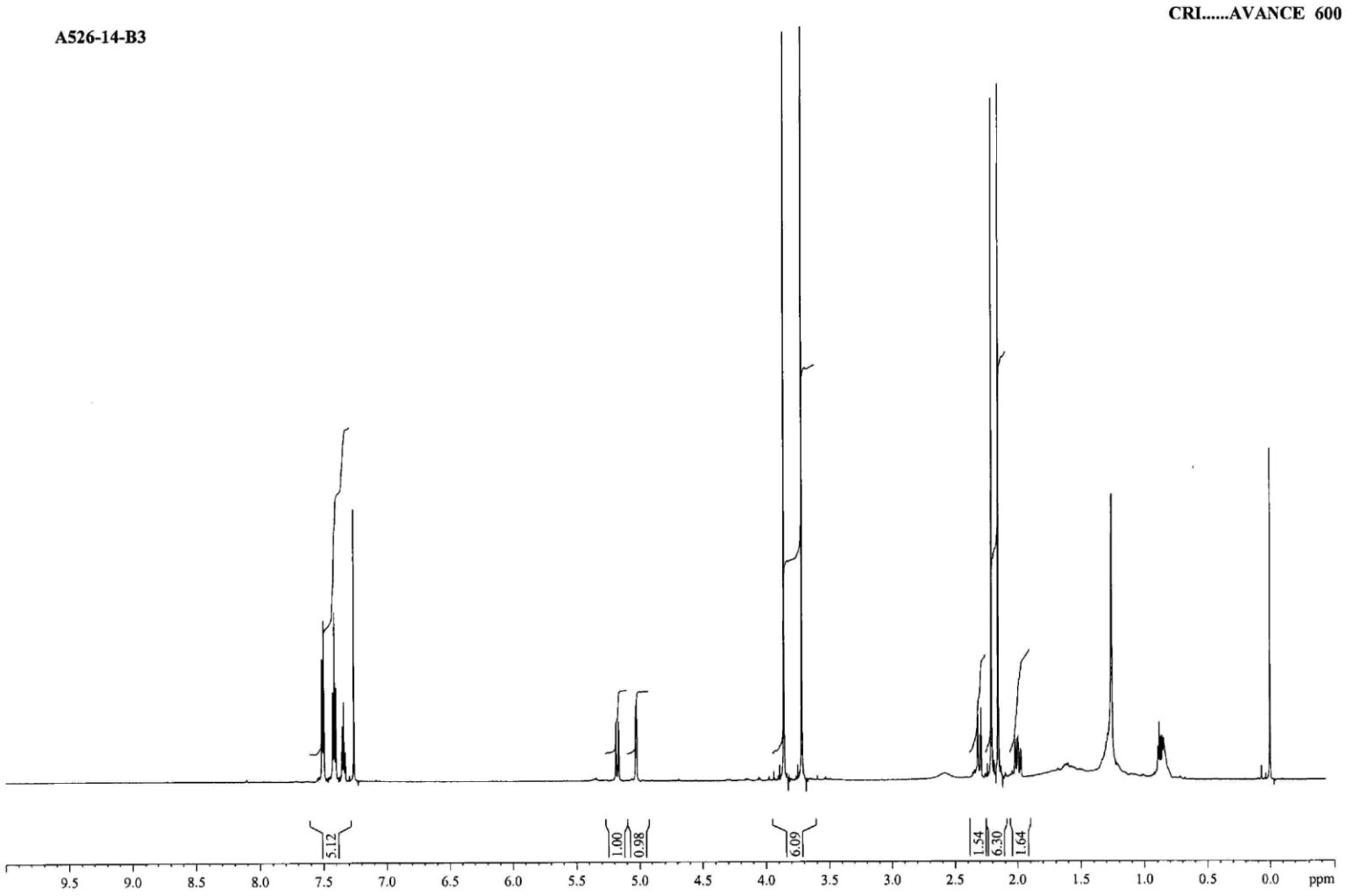

Fig. S12. ^{13}C NMR spectrum ($CDCl_3$) of compound **3**

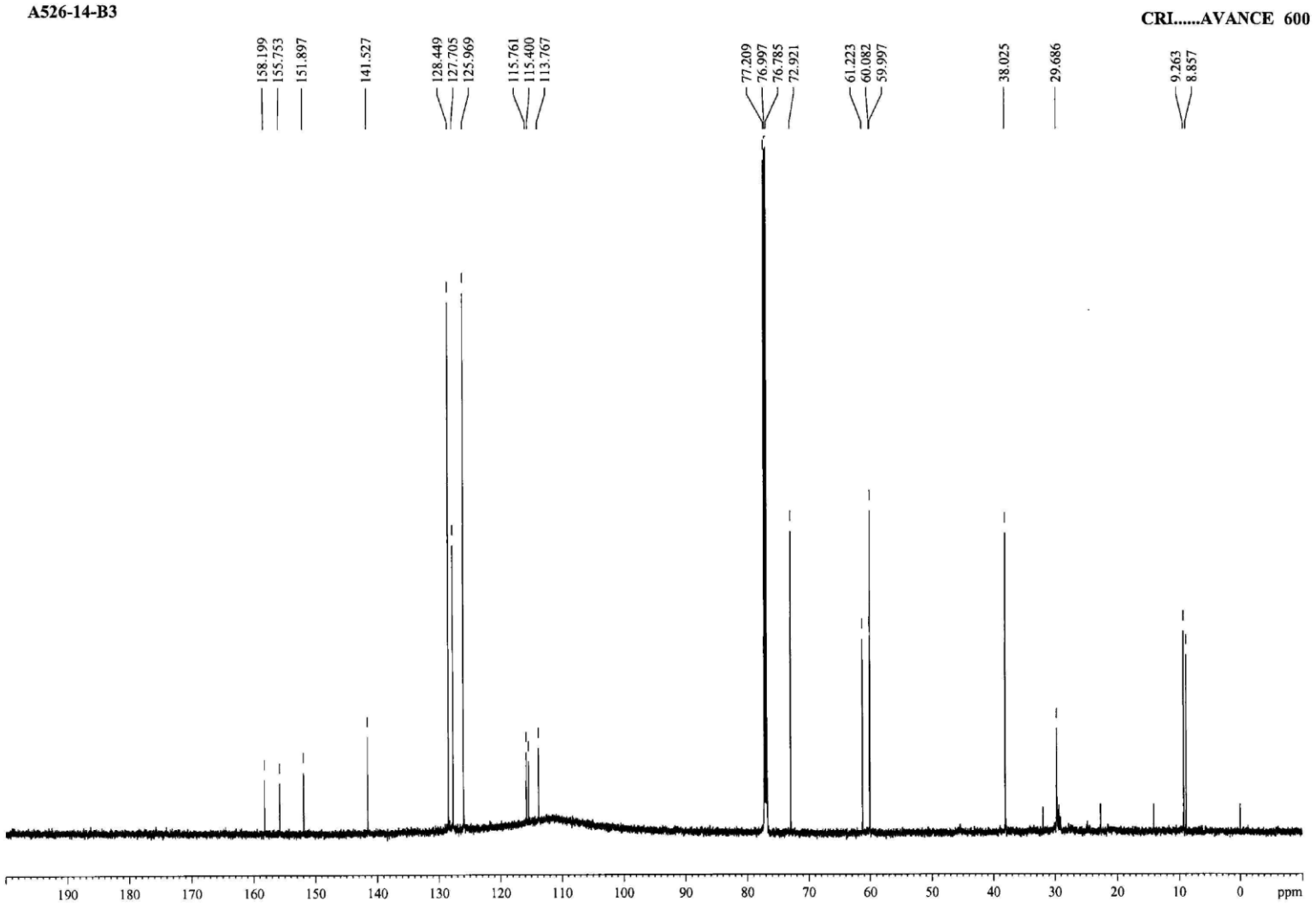

Fig. S13. HMQC spectrum of compound **3**

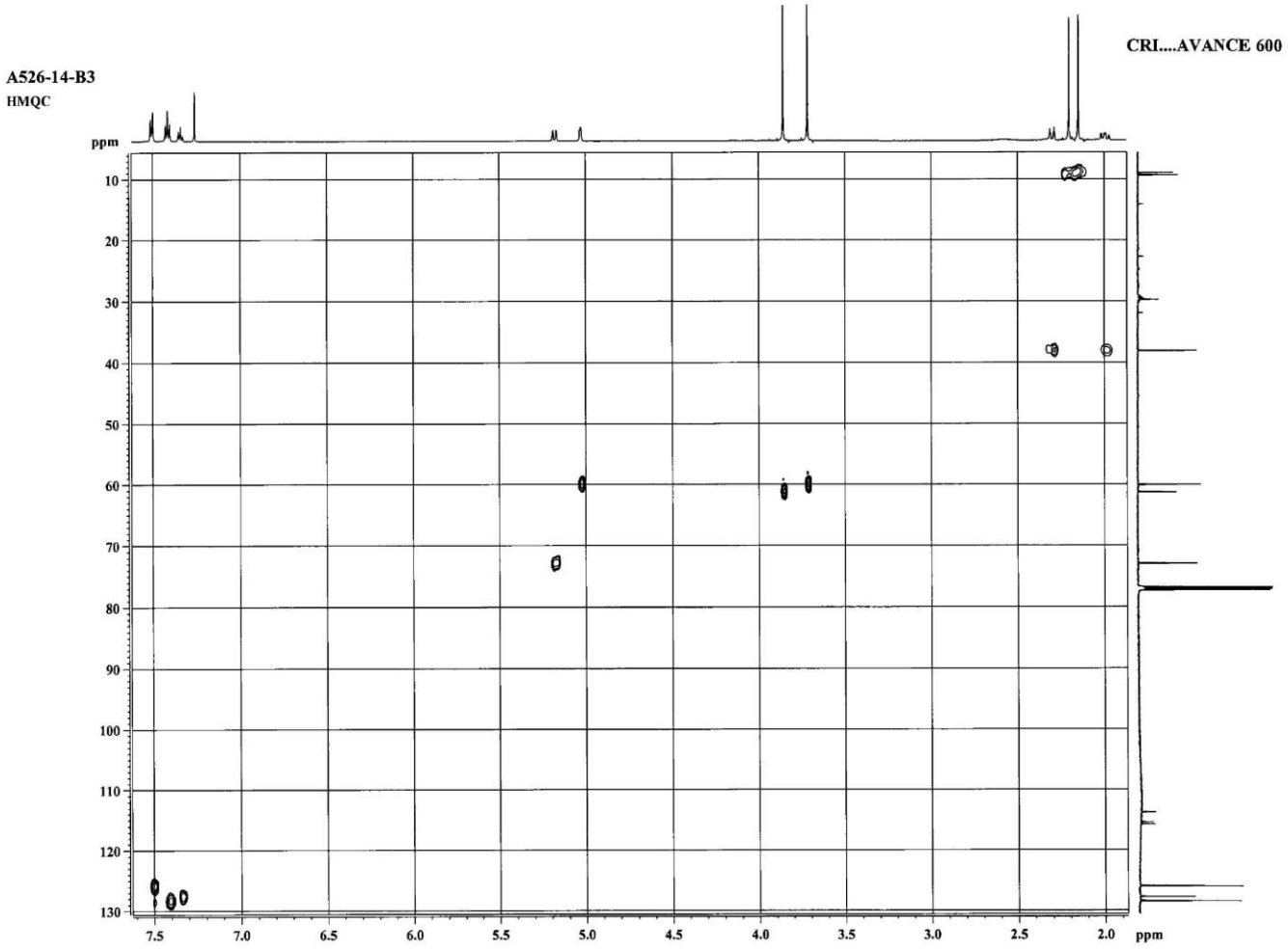

Fig. S14. HMBC spectrum of compound **3**

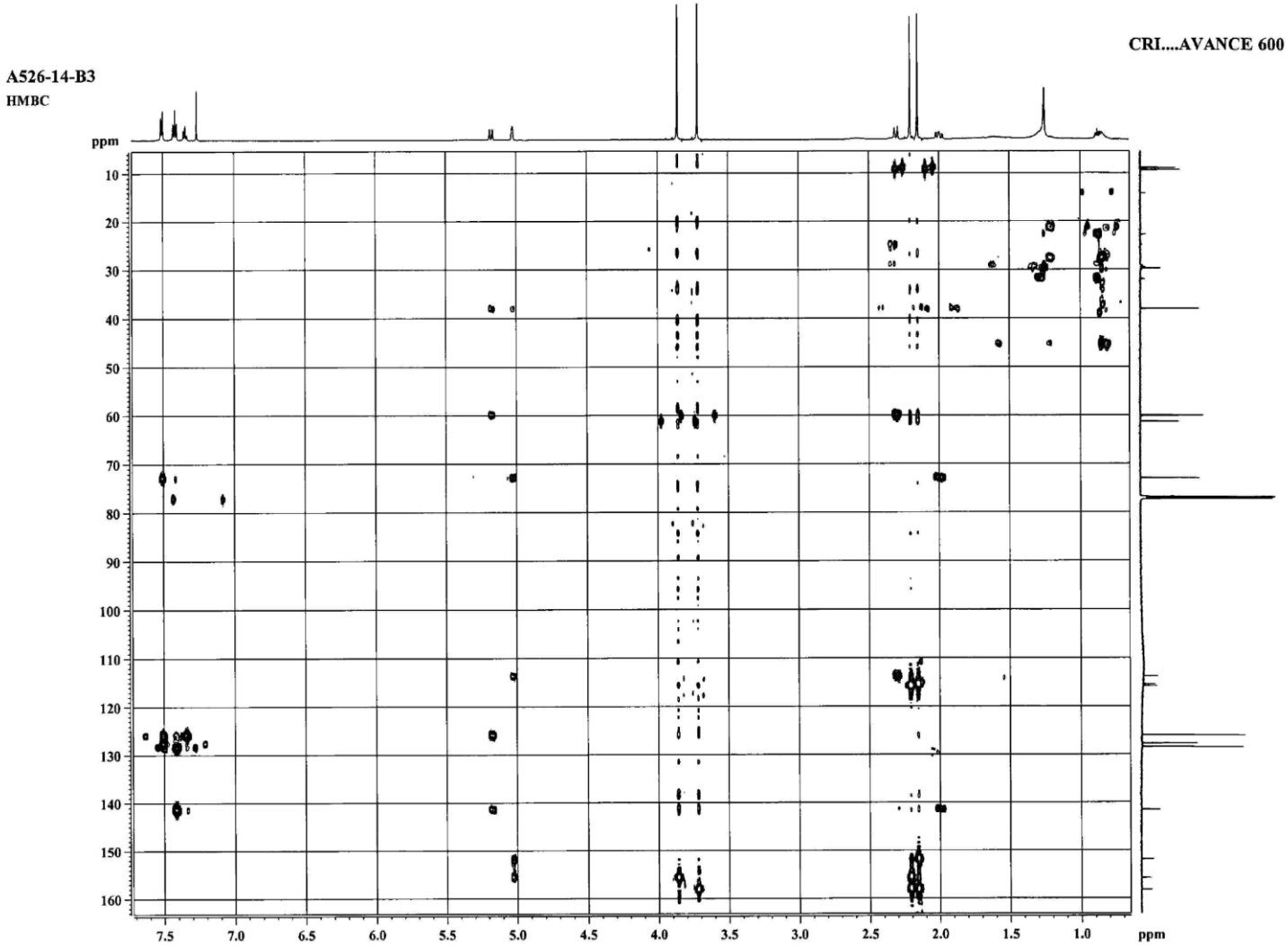

Fig. S15. ^{1}H NMR spectrum ($CDCl_3$) of compound **4**

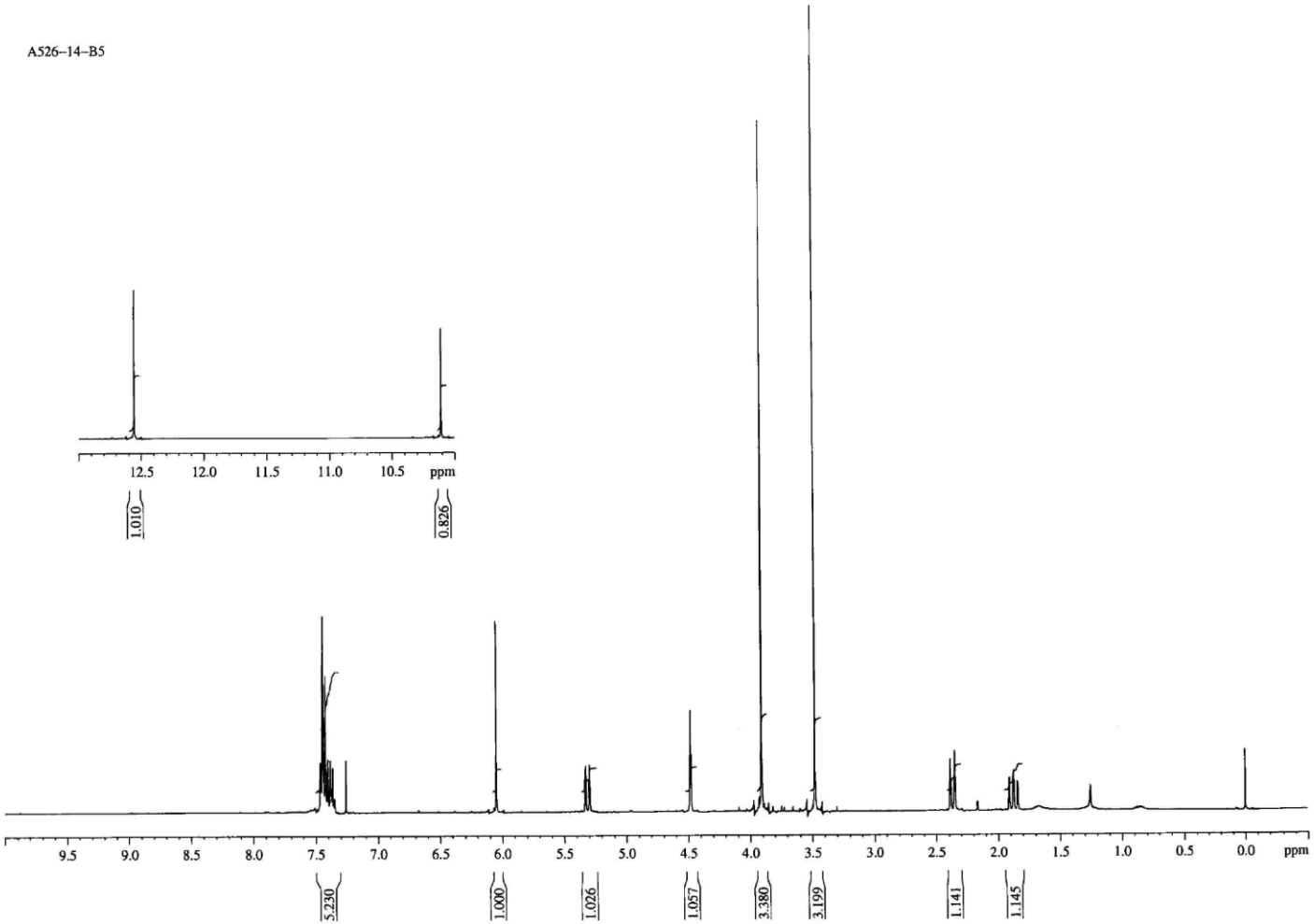

Fig. S16. ^{13}C NMR spectrum ($CDCl_3$) of compound **4**

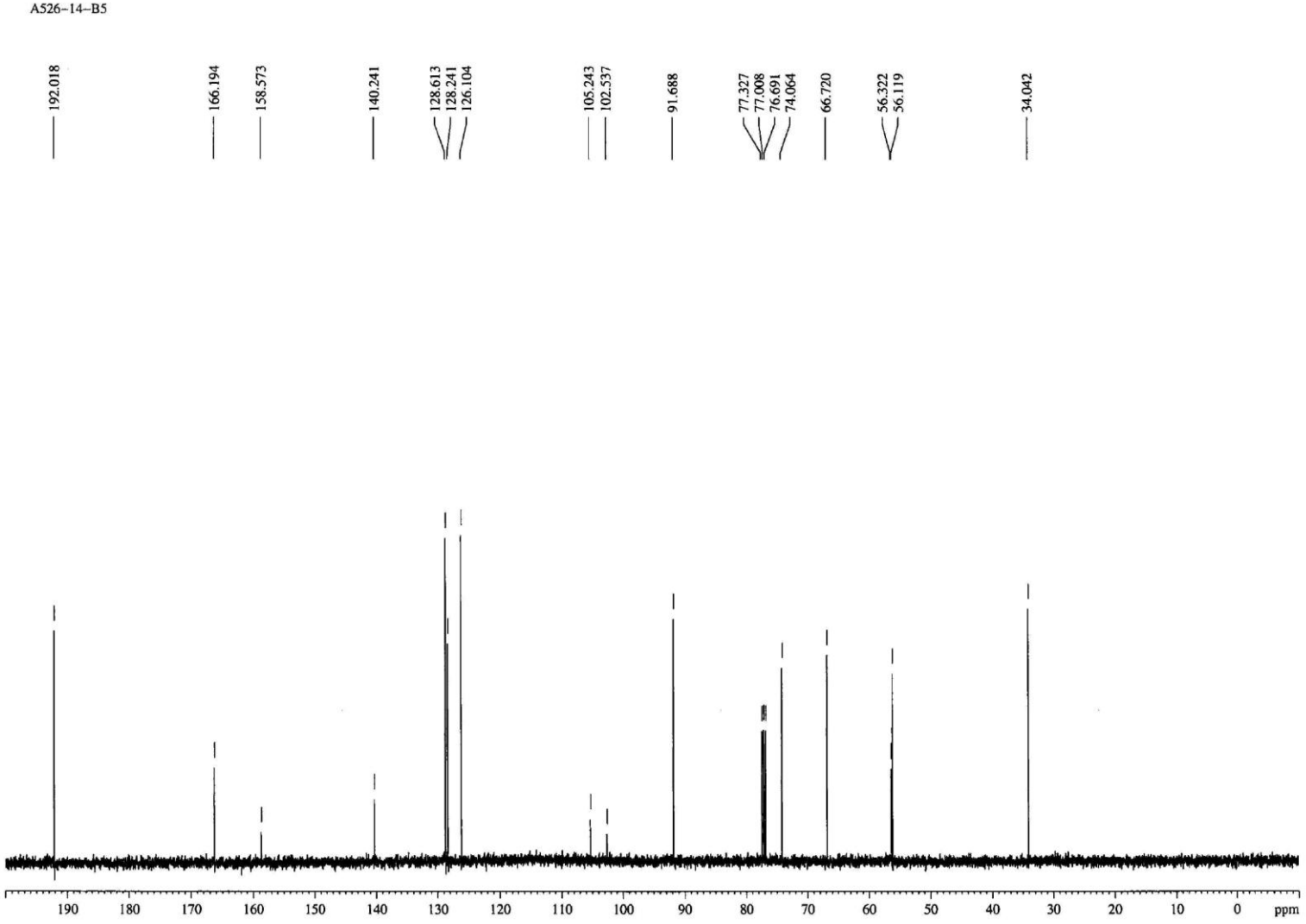

Fig. S17. HMQC spectrum of compound **4**

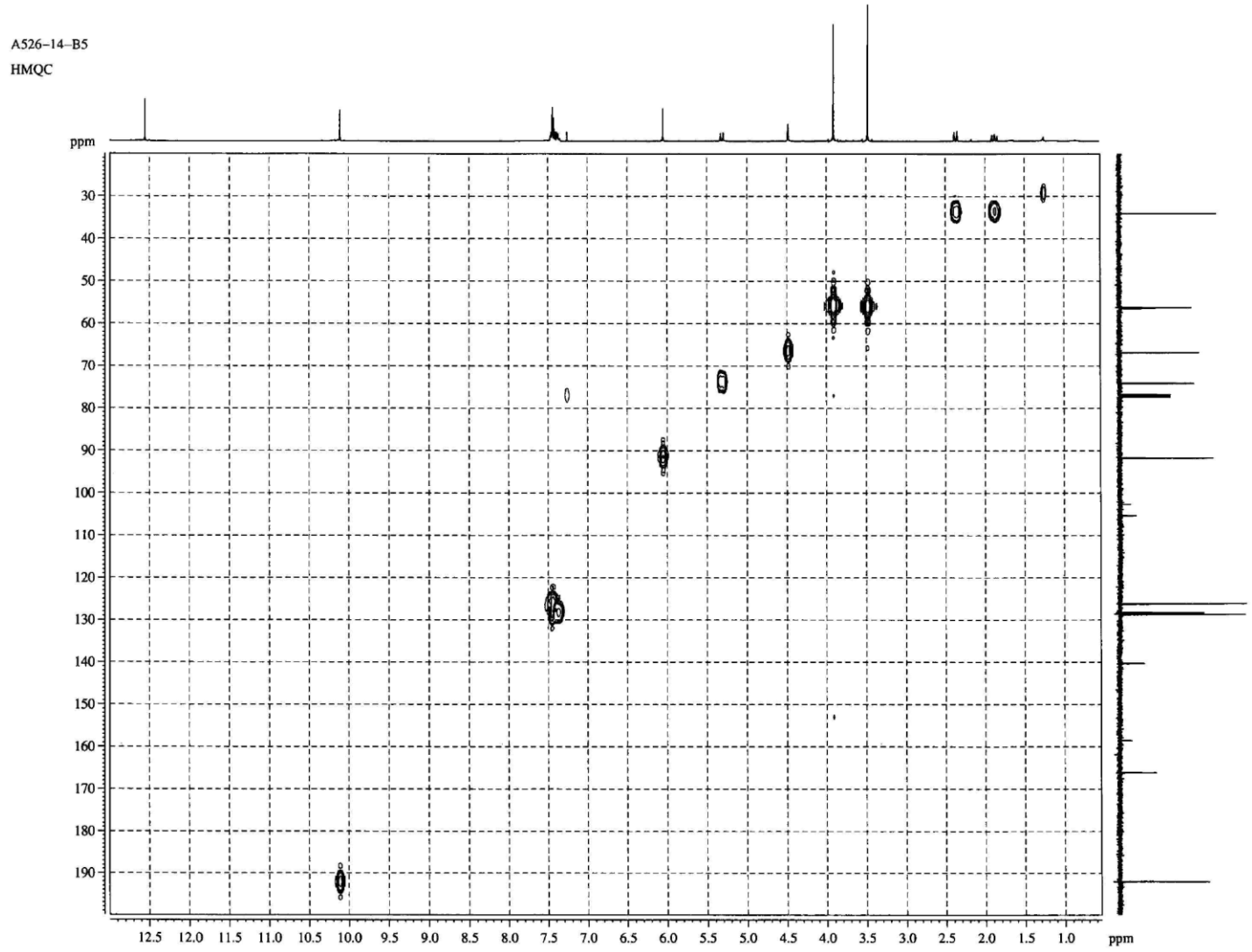

Fig. S18. HMBC spectrum of compound **4**